Author/s:
Warren, AEL;Harvey, AS;Abbott, DF;Vogrin, SJ;Bailey, C;Davidson, A;Jackson, GD;Archer, JS

Title:
Cognitive network reorganization following surgical control of seizures in Lennox-Gastaut syndrome

Date:
2017-05-01

Citation:
Warren, A. E. L., Harvey, A. S., Abbott, D. F., Vogrin, S. J., Bailey, C., Davidson, A., Jackson, G. D. & Archer, J. S. (2017). Cognitive network reorganization following surgical control of seizures in Lennox-Gastaut syndrome. Epilepsia, 58 (5), pp.e75-e81. https://doi.org/10.1111/epi.13720.

Persistent Link:
https://hdl.handle.net/11343/292633

Received Date : 21-Sep-2016

Revised Date : 12-Feb-2017

Accepted Date : 12-Feb-2017

Article type : Brief Communication (includes Case Reports)

Cognitive network reorganization following surgical control of seizures in Lennox-Gastaut syndrome

Aaron E.L Warren[1,5], A. Simon Harvey[2,4,5,7], David F. Abbott[1,2], Simon J. Vogrin[5], Catherine Bailey[4], Andrew Davidson[5,6,7], Graeme D. Jackson[1,2,3], John S. Archer[1,2,3,5]

[1]Department of Medicine, The University of Melbourne, Victoria, Australia

[2]The Florey Institute of Neuroscience and Mental Health, The University of Melbourne, Victoria, Australia

[3]Department of Neurology, Austin Health, Victoria, Australia

[4]Department of Neurology, The Royal Children's Hospital, Victoria, Australia

[5]Murdoch Childrens Research Institute, Victoria, Australia

[6]Department of Anaesthesia and Pain Management, The Royal Children's Hospital, Victoria, Australia

[7]Department of Paediatrics, The University of Melbourne, Victoria, Australia

Contact information:

Name: Aaron Warren

Address: Melbourne Brain Centre, 245 Burgundy Street, Heidelberg, VIC, 3084,

E-mail: a.warren@brain.org.au

Phone number: +61 3 9035 7110

Running title: Post-surgical network changes in LGS

Keywords: Lennox-Gastaut syndrome, epileptic encephalopathy, surgery, fMRI, graph theory

Text pages: 15

Summary: 200 words

Manuscript body: 2099 words

References: 18

Figures: 2 (+2 supplementary)

Supplementary Tables: 1

Summary

We previously observed that adults with Lennox-Gastaut syndrome (LGS) show abnormal functional connectivity among cognitive networks, suggesting this may contribute to impaired cognition. Here we report network reorganization following seizure remission in a child with LGS who underwent functional MRI (fMRI) before and after resection of a cortical dysplasia.

Concurrent EEG was acquired during pre-surgical fMRI. Pre- and post-surgical functional connectivity were compared using i) graph theoretical analyses of small-world network organization and node-wise strength; and ii) seed-based analyses of connectivity within and between five functional networks. To explore the specificity of these post-surgical network changes, connectivity was further compared to nine children with LGS who did not undergo surgery.

The pre-surgical EEG-fMRI revealed diffuse activation of association cortex during interictal discharges. Following surgery and seizure control, functional connectivity showed increased small-world organization, stronger connectivity in sub-cortical structures, and greater within-network integration/between-network segregation. These changes suggest network improvement, and diverged sharply from the comparison group of non-operated children.

Following surgery, this child with LGS achieved seizure control and showed extensive reorganization of networks that underpin cognition. This case illustrates that the epileptic process of

LGS can directly contribute to abnormal network organization, and that this network disruption may be reversible.

Keywords: Lennox-Gastaut syndrome, epileptic encephalopathy, surgery, fMRI, graph theory

Introduction

Lennox-Gastaut syndrome (LGS) is an epileptic encephalopathy of childhood characterized by multiple seizure types, including tonic seizures, and generalized epileptic activity on EEG[1]. Frequent epileptic activity is thought to contribute to impaired cognition in this syndrome[2]. More than 80% of LGS patients have pharmacoresistant seizures and intellectual disability[1]. However, removal of an epileptogenic cortical lesion can lead to seizure remission and developmental gains[3-7].

Our recent studies using EEG with concurrent fMRI (EEG-fMRI) showed that interictal epileptiform discharges in LGS engage distributed networks that normally support cognitive processes, including the default-mode (DMN) and dorsal attention (DAN) networks[7,8]. These findings are similar across patients with[7] and without[8] cortical lesions in diverse locations, suggesting that LGS may involve shared network dysfunction that is 'secondary' to the underlying cause of epilepsy[9].

If LGS remains poorly controlled, epileptic activity likely imprints enduring patterns of abnormal network organization. Adults with longstanding LGS show abnormal fMRI connectivity among networks involved in the expression of discharges, including reduced within-DMN integration and impaired DMN/DAN segregation[10]. fMRI studies using graph theoretical analysis have identified several properties that facilitate efficient communication of brain regions ("nodes") via their pairwise functional covariance ("edges")[11]. In particular, the healthy brain shows a 'small-world' organization that balances competing demands for local node clustering and global node integration[12].

We hypothesized that surgical control of seizures in LGS would permit improvements in functional network organization. Pre- and post-surgical anesthetized fMRI data were acquired in a child with LGS who achieved seizure remission after resection of a cortical dysplasia. Concurrent EEG was acquired during the pre-surgical scan to assess correspondence with prior EEG-fMRI observations

in older LGS patients[7,8]. Post-surgical network changes were explored using seeded connectivity and graph theoretical analyses. Additionally, we explored the specificity of the patient's post-surgical network changes by anesthetized fMRI in a comparison group of non-operated children with LGS.

Methods

Patients

This report describes a surgical patient (case subject) and a group of nine non-operated patients (comparison group), all of whom had LGS[1] defined by i) tonic seizures, ii) slow spike-and-wave (SSW) and generalized paroxysmal fast activity (GPFA) on interictal EEG, and iii) intellectual disability. The case subject underwent pre-surgical scanning at age 2.7 years (two months before surgery) and post-surgical scanning at age 5.6 years (2.7 years after surgery). The nine children (six females) who did not undergo surgery were scanned at a mean age of 10.5 years (range: 4.3-15 years). Clinical information for the case subject is described below, and for the comparison group in Supplementary Table 1. Patients were recruited through the Royal Children's Hospital (RCH), Melbourne. fMRI was added to each patient's clinically-requested MRI session after written informed consent was given by their legal guardian. Before recruitment began, this study was approved by the RCH human research ethics committee.

Surgical case subject

The case subject was a boy with LGS secondary to a left temporal lobe dysplasia (type 1) involving the left parahippocampal, fusiform, and hippocampal gyri (Figure 1a). Seizure onset occurred at age 1.2 years and was associated with developmental regression, including loss of previously acquired single-word utterances. Video-EEG monitoring revealed generalized tonic seizures. Interictal EEG showed left temporal sharp-slow discharges, lateralized and generalized SSW, and GPFA. He was prescribed lamotrigine, sodium valproate, clobazam, levetiracetam, vigabatrin and topiramate, prior to undergoing a left anterior-medial temporal lobectomy at age 2.9 years. After surgery, he experienced seizure remission and scalp EEG normalization (Figure 1a). Anti-epileptic medications were discontinued at age 3.9 years. Pre-surgical adaptive functioning at age 2.7 years was rated at a 7-12 month old level, with no language. Post-surgically, at age 8.5 years, he has an intellectual disability but has developed some language with two-word utterances.

MRI acquisition under general anesthesia

fMRI data were acquired in a 3 tesla Siemens Trio MRI scanner (TR=3,200 ms; TE=40 ms; 3.4 mm^3 voxels). 30 minutes of data were acquired for each patient, with the exception of the case subject's post-surgical scan, for which 15 minutes were acquired. For the pre-surgical EEG-fMRI analysis, we used the case subject's complete data; for other analyses, we used only the first 15 minutes of each patient's scan. A T1 image was acquired for each patient. Due to their young age and intellectual disability, all patients were scanned under general anesthesia. During the case subject's pre- and post-surgical scans, anesthesia was maintained with low-dose inhaled isoflurane (end-tidal concentration=0.3%) and intravenous remifentanil (range=0.05-0.1 mcg/kg/min). In the comparison group, anesthesia was maintained using identical agents (isoflurane, range: 0.2-0.8%; remifentanil, range: 0.02-0.1 mcg/kg/min). At these dosages, isoflurane and remifentanil have minimal influence on patients' intrinsic EEG patterns[13,14]. We use this anesthetic regimen during epilepsy surgery at our center, as the appearance of interictal epileptiform discharges during electrocorticography is similar to that seen during sleep.

Pre-surgical EEG-fMRI

All patients had concurrent 64-channel scalp EEG (Compumedics Neuroscan) acquired during fMRI. Only the case subject's pre-surgical EEG-fMRI analysis is reported here. Analysis was performed in the subject's native brain space using Statistical Parametric Mapping (SPM8), as previously described[7,8]. For each discharge type identified on the in-scanner EEG, event onsets/durations were convolved with SPM8's hemodynamic response function. Significant fMRI changes were assessed using two-tailed one-sample *t*-tests (cluster-level $p<0.05$ false-discovery-rate correction following a voxel-wise feature selection threshold of $p<0.001$ uncorrected).

fMRI pre-processing for connectivity analyses

fMRI pre-processing is detailed in Supplementary Information. Briefly, each patient's fMRI data were temporally interpolated to yield a uniform slice acquisition, spatially realigned to the middle volume, co-registered with each patient's T1, and warped to a custom template constructed using a database of healthy pediatric T1 images[15]. De-noising steps included i) removing variance attributable to head motion and white matter/CSF; ii) removing each volume with frame-wise displacement >0.5 mm, as well as the following two volumes; and iii) temporal frequency filtering

(0.01-0.1 Hz). Spatial smoothing was performed using a Gaussian kernel with full-width-at-half-maximum=6 mm.

Weighted graph construction and analysis

An analysis mask (Figure 2c) was created by segmenting grey matter from the custom template. The mask was restricted to the right hemisphere to ensure common coverage by avoiding distortions on the case subject's left brain side caused by the resection and a post-surgical CSF collection (Figure 1a). The mask was randomly partitioned into 1,024 nodes[16]. A weighted graph was constructed for each patient with edges defined using positive Pearson correlations between mean node timecourses. Graphs were thresholded to include only the strongest 23% of edges; this was the minimum density at which all nodes in each graph comprised a single connected component. Weighted graph metrics were computed using the Brain Connectivity Toolbox (https://sites.google.com/site/bctnet/):

Network analysis: Small-world organization was assessed using the metrics of characteristic path length and mean clustering coefficient[11]. Metrics were normalized with reference to random ('null') models with an equivalent number of nodes/edges and preserved degree distribution[11]. Small-world organization was calculated as the ratio of mean clustering coefficient to characteristic path length.

Node analysis: Node-level connectivity changes were assessed by comparing strength[11] of each node in the case subject's pre- and post-surgical graphs. Differences were considered clinically significant if they exceeded one SD of the mean change in strength across all nodes (i.e., $Z>1$ and $Z<-1$).

Seeded functional connectivity

Functional connectivity was assessed using spherical seeds (radius=6 mm) placed within five networks of interest (Supplementary Figure 1 shows seed locations). Connectivity was determined using the Pearson correlation between mean fMRI timecourses within each seed pair.

Results

Pre-surgical EEG-fMRI

106 GPFA events (cumulative duration=92.5 secs) were identified during the case subject's pre-surgical EEG-fMRI (Figure 1b). Prominent bilateral activation was observed in frontal, temporal, parietal, and cingulate cortex; and the caudate, ventral striatum, thalamus, and pons. Bilateral deactivation was observed in primary motor, visual, and auditory cortex; and the hippocampus, parrahippocampal cortex, and cerebellum. Interestingly, the patient's lesion did not show significant activation. 145 generalized polyspike-wave events (cumulative duration=43.5 secs) were also identified, which showed fMRI changes similar to the GPFA analysis (Supplementary Figure 2).

Post-surgical increase in network integration and segregation

Seeded connectivity matrices are displayed in Figure 2a. On visual inspection, the average connectivity pattern in the comparison group was more like the case subject's pre-surgical scan than the post-surgical scan: both the comparison group's matrix and the case subject's pre-surgical matrix showed weakly positive within-network connectivity, and positive between-network connectivity. In contrast, the case subject's post-surgical matrix showed stronger positive within-network connectivity, and a more extensive pattern of negative between-network connectivity.

Post-surgical increase in small-world organization

Pre-surgically, the case subject's characteristic path length and mean clustering coefficient were within one SD of the mean values for the comparison group (Figure 2b). Post-surgically, a strong increase in clustering was observed (>2 SD above the comparison group mean), while path length remained relatively stable (within 1 SD of the comparison group mean). This was associated with a strong post-surgical increase in small-world organization (>2 SD above the comparison group mean).

Post-surgical changes in node-level connectivity strength

Post-surgically, decreased strength was most prominent in association cortex (including frontal, temporal, and parietal regions), and was also observed in the caudate and ventral striatum (Figure 2c). Increased strength was maximal sub-cortically (including cerebellum, hippocampus, brainstem, and thalamus), and was also seen in the middle frontal gyrus, lingual gyrus, and cuneus.

Discussion

In the case subject, removal of the dysplasia was associated with seizure remission and extensive functional reorganization of the non-operated hemisphere. On visual inspection, pre-surgical seeded connectivity showed broad similarity to the average pattern in the comparison group of non-operated LGS children as well as our prior observations in non-anesthetized LGS adults[10], including: positive connectivity between networks that are normally anti-correlated (e.g., the DMN and DAN)[10,17], and weakly positive connectivity between distant nodes within networks that are normally strongly correlated (e.g., anterior and posterior areas of the DMN)[10,17]. Post-surgically, there was greater between-network negative connectivity and stronger within-network positive connectivity, a pattern that more closely resembles network behavior typically seen in healthy children[17] and adults[10].

Pre-surgical EEG-fMRI revealed significant discharge-related activation in distributed areas of association cortex that normally support key cognitive processes (including frontal, temporal, and parietal cortex), while the patient's lesion did not show significant activation. This pattern is similar to our prior EEG-fMRI observations in non-anesthetized adults with longstanding LGS[7,8], illustrating that network expression of epileptic activity can be identifiable at an early stage in the syndrome's evolution, and can be studied under our anesthetic regimen, which did not suppress discharges.

Following surgery, a strong increase in mean clustering coefficient occurred, while characteristic path length remained stable, indicating a departure from a random to small-world network topology[11,12]. This shift diverged sharply from the comparison group of non-operated children with LGS of various ages, implying the post-surgical improvement was not merely age-related. At a regional level, post-surgical *decreases* in connectivity strength were most prominent in association cortical areas that showed pre-surgical discharge-related EEG-fMRI activation. In contrast, post-surgical *increases* in connectivity strength were maximal sub-cortically, suggesting that seizure control may permit a more optimal balance between cortical and sub-cortical connectivity load[12].

Limitations and future directions

A larger surgical cohort is required to determine generalizability of this observation to other LGS patients. Results may have been influenced by variation to the case subject's anti-epileptic medications, which were discontinued following surgery. However, prior fMRI studies show that abnormal connectivity persists in drug-naïve children with generalized epilepsy[18], implying that medication discontinuation is unlikely to be solely responsible for the case subject's network

changes. Although scanning occurred under general anesthesia, which may affect fMRI connectivity, all studies utilized identical anesthetic agents, and thus this factor alone does not account for the post-surgical network changes. Comparison to healthy control subjects was not possible given the need for anesthesia in these patients. However, we did compare the case subject to a group of non-operated patients who were matched with respect to their diagnosis of LGS and anesthetic agents used during scanning. Results from this non-operated comparison group (which included children of similar age to, as well as older than, the case subject's post-surgical scan) suggest that the case subject's network changes following surgery are unlikely to be only age-related. However, future studies exploring the influence of age on network organization in LGS will be important. Additionally, while post-surgical network changes were associated with seizure control, the relevance of improved network organization to neuropsychological outcomes requires further studies.

Conclusions

Our report provides one example of a case where interruption of the epileptic process in LGS by early surgical intervention led to functional reorganization of brain networks underpinning cognition. Given the marked divergence of these network changes from non-operated children and adults[10] with LGS, we hypothesize that early seizure control may restore network maturational trajectories, perhaps contributing to the modest developmental gains reported in some operated patients[3-6].

Acknowledgements

We thank the patients and their families for participating in this research. We also thank Michael Kean for coordinating MRI scanning. This study was supported by the National Health and Medical Research Council of Australia (NHMRC), project grant number 628725 (John S. Archer and David F. Abbott) and practitioner fellowship number 1060312 (Graeme D. Jackson). Aaron E.L. Warren is supported by an Australian Government Research Training Program Scholarship. David F. Abbott is supported by a National Imaging Facility Fellowship. We acknowledge the facilities and the scientific and technical assistance of the National Imaging Facility at the Florey node, and the support of the Victorian Government through the Operational Infrastructure Support Grant.

Disclosure of conflicts of interest

None of the authors has any conflict of interest relevant to this research activity to disclose. We confirm that we have read the Journal's position on issues involved in ethical publishing and affirm that this report is consistent with those guidelines.

References

1. Arzimanoglou A, French J, Blume WT, et al. Lennox-Gastaut syndrome: a consensus approach on diagnosis, assessment, management, and trial methodology. Lancet Neurol. 2009;8:82-93.
2. Howell KB, Harvey AS, Archer JS. Epileptic encephalopathy: Use and misuse of a clinically and conceptually important concept. Epilepsia. 2016;57:343-7.
3. Gupta A, Chirla A, Wyllie E, Lachhwani DK, Kotagal P, Bingaman WE. Pediatric epilepsy surgery in focal lesions and generalized electroencephalogram abnormalities. Pediatr Neurol. 2007;37:8-15.
4. Freeman J, Harvey A, Rosenfeld J, et al. Generalized epilepsy in hypothalamic hamartoma Evolution and postoperative resolution. Neurology. 2003;60:762-7.
5. Wyllie E, Lachhwani D, Gupta A, Chirla A, Cosmo G, Worley S, et al. Successful surgery for epilepsy due to early brain lesions despite generalized EEG findings. Neurology. 2007;69:389-97.
6. Pizoli CE, Shah MN, Snyder AZ, et al. Resting-state activity in development and maintenance of normal brain function. Proc Natl Acad Sci U S A. 2011;108:11638-43
7. Archer JS, Warren AEL, Stagnitti MR, et al. Lennox-Gastaut Syndrome and Phenotype: secondary network epilepsies. Epilepsia. 2014;55:1245-54.
8. Pillay N, Archer JS, Badawy RA, et al. Networks underlying paroxysmal fast activity and slow spike and wave in Lennox-Gastaut syndrome. Neurology. 2013;81:665-73.
9. Archer JS, Warren AEL, Jackson GD, et al. Conceptualising Lennox-Gastaut Syndrome as a secondary network epilepsy. Front Neurol. 2014;5:1-11.
10. Warren AEL, Abbott DF, Vaughan DN, et al. Abnormal cognitive network interactions in Lennox-Gastaut Syndrome: A potential mechanism of epileptic encephalopathy. Epilepsia. 2016;57:812-22.
11. Rubinov M, Sporns O. Complex network measures of brain connectivity: uses and interpretations. Neuroimage. 2010;52:1059-69.
12. Stam CJ. Modern network science of neurological disorders. Nat Rev Neurosci. 2014;15:683-95.
13. Herrick IA, Craen RA, Blume WT, et al. Sedative doses of remifentanil have minimal effect on ECoG spike activity during awake epilepsy surgery. J Neurosurg Anesthesiol. 2002;14:55-8.

14. Fiol ME, Boening JA, Cruz-Rodriguez R, et al. Effect of isoflurane (Forane) on intraoperative electrocorticogram. Epilepsia. 1993;34:897-900.
15. Richards JE, Sanchez C, Phillips-Meek M, et al. A database of age-appropriate average MRI templates. Neuroimage. 2015;124:1254-9.
16. Zalesky A, Fornito A, Harding IH, et al. Whole-brain anatomical networks: does the choice of nodes matter? Neuroimage. 2010;50:970-83.
17. Chai XJ, Ofen N, Gabrieli JD, et al. Selective Development of Anticorrelated Networks in the Intrinsic Functional Organization of the Human Brain. J Cogn Neurosci. 2014;26:501-13.
18. Yang T, Luo C, Li Q, et al. Altered resting-state connectivity during interictal generalized spike-wave discharges in drug-naïve childhood absence epilepsy. Hum Brain Mapp. 2013;34:1761-7.

Figure legends

Figure 1:

a) The case subject's pre- and post-surgical T1-weighted MRI and routine clinical scalp EEG findings. **Left:** Pre-surgical MRI revealed a type 1 left temporal lobe dysplasia (green box). Routine awake/asleep EEG revealed both focal (including left temporal) and generalized interictal epileptiform discharges characteristic of LGS. **Right:** Following a left anterior-medial

temporal lobectomy, the case subject experienced seizure remission and a return of normal awake/asleep EEG architecture.

b) The case subject's pre-surgical anesthetized EEG-fMRI revealed discharge-related signal changes similar to previously observed patterns in non-anesthetized adults with LGS[7,8]. **Left:** fMRI activation (red-yellow) and deactivation (blue-light blue) associated with generalized paroxysmal fast activity (GPFA). Results are displayed on the subject's T1 image as *t*-scores thresholded at $p<0.05$ (cluster-corrected using the false-discovery-rate, two-tailed). The green arrows indicate the subject's left medial temporal dysplasia. **Right:** In-scanner EEG sample showing GPFA.

Figure 2:

a) Seeded functional connectivity matrices, displayed separately for i) mean connectivity in the comparison group of non-operated children with LGS (far left), ii) the case subject's pre-surgical connectivity (middle), and iii) the case subject's post-surgical connectivity (far right). Each matrix square represents the Pearson correlation (Fisher's *r*-to-*z* transformed) between the timecourses of each seed pair displayed along *x* and *y* axes (red=positive connectivity; blue=negative connectivity). Seeds are grouped according to five functional networks of interest (PC=primary cortical; ASN=anterior-salience network; DMN=default-mode network; DAN=dorsal-attention network; ECN=executive-control network). See Supplementary Figure 1 for anatomical seed locations.

b) Weighted graph theoretical analysis of normalized network-level metrics (mean clustering coefficient, characteristic path length, small-world organization) displayed separately for the case subject's pre-surgical (red bars) and post-surgical (green bars) scans, along with the mean values (±1 standard deviation) for the comparison group of non-operated children with LGS (grey bars). The dotted horizontal line represents the equivalent values of each metric in random (null) network models.

c) Differences in node-level connectivity strength between the case subject's pre- and post-surgical scans (red-yellow=post-surgical increases in strength; blue-light blue=post-surgical decreases in strength), displayed as *z*-scores reflecting the distance (in units of standard deviation) from the mean change in strength across all nodes. Analysis was restricted to grey matter on the right (i.e., non-operated) brain side, as shown by the mask in purple. Results are thresholded at $z<-1$ and $z>1$ to show nodes with the greatest post-surgical change in strength, and are displayed on a custom pediatric brain template constructed from a database of age-appropriate healthy T1 images[15].

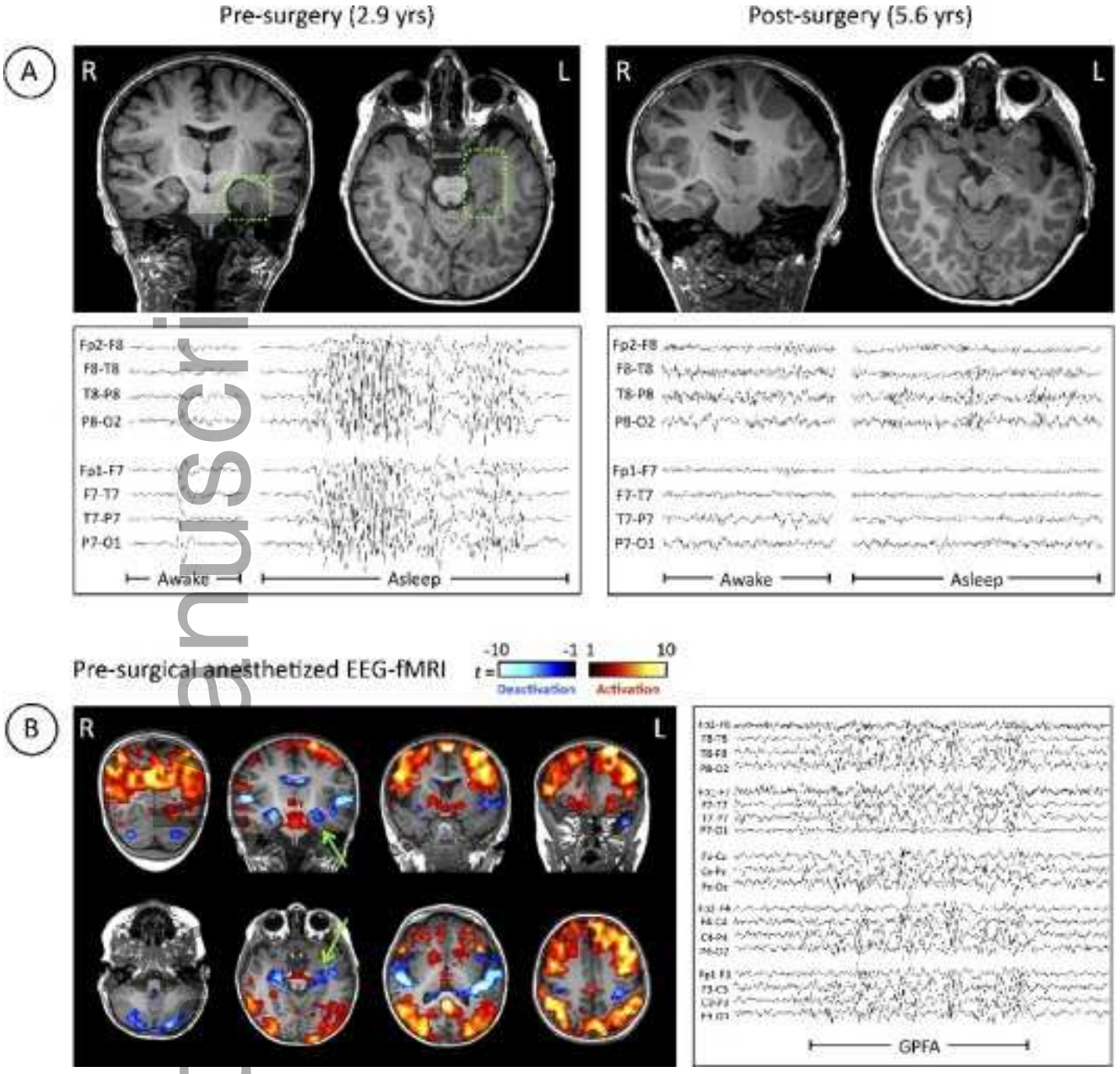

epi_13720_f1.tiff

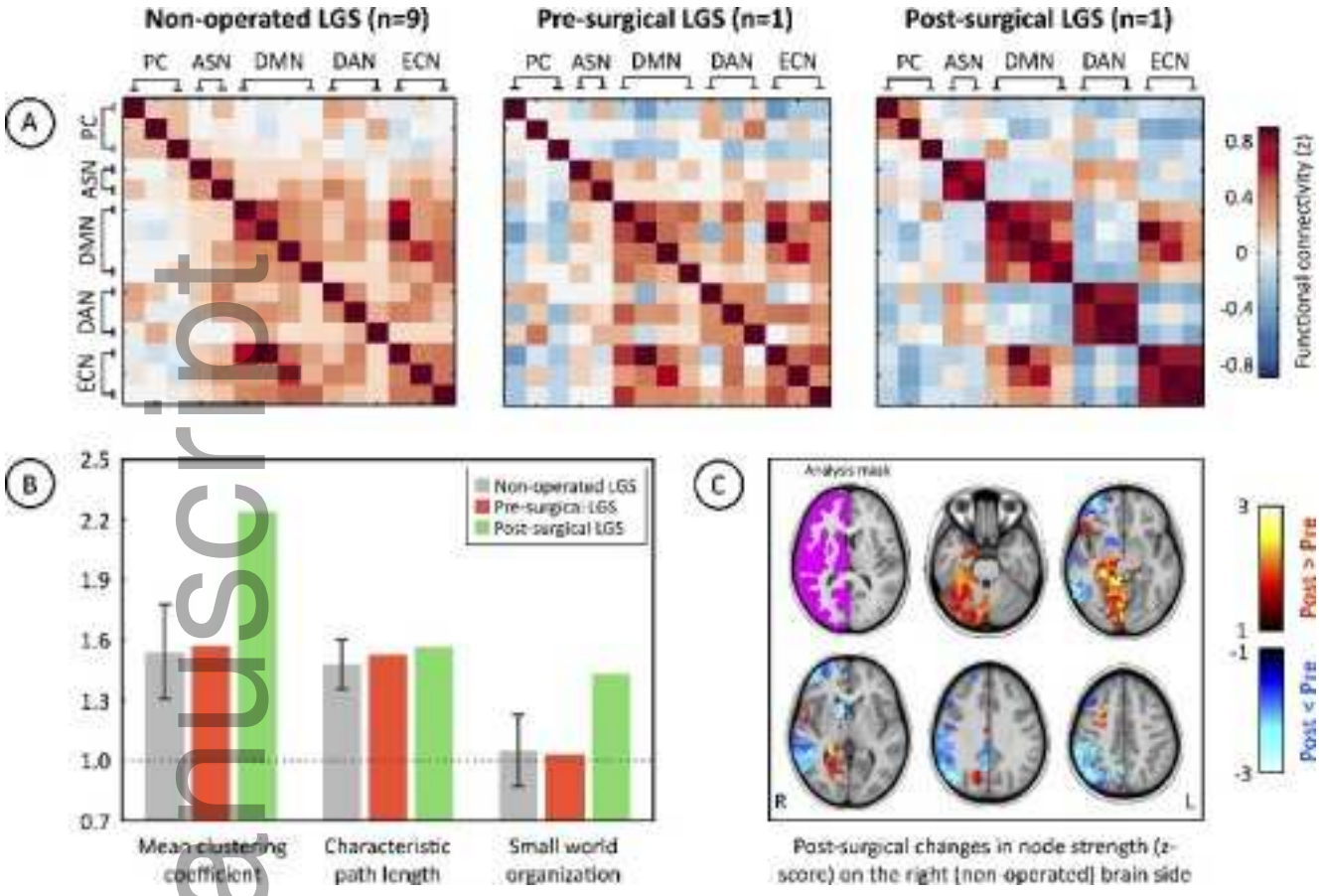

epi_13720_f2.tiff